

Gold(I) Complex with a Photoactive Ligand Behaves as a Two-in-One Dual Metallaphotoredox Cross-Coupling Catalyst

César Ruiz-Zambrana, Macarena Poyatos,* and Eduardo Peris*



Cite This: *ACS Catal.* 2024, 14, 4066–4073



Read Online

ACCESS |



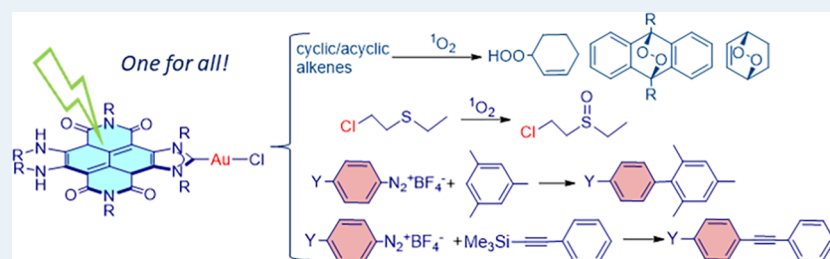
Metrics & More



Article Recommendations



Supporting Information



ABSTRACT: We herein describe the use of a gold complex with a naphthalene-di-imide-functionalized N-heterocyclic carbene (NDI-NHC) ligand, which was used as a photocatalyst for a variety of reactions. Due to the presence of the naphthalene moiety in the ligand, the complex can be used for the photogeneration of singlet oxygen, behaving as a photocatalyst in the endoperoxidation and peroxidation of cyclic and acyclic alkenes, and also in the selective oxidation of a simulant of sulfur mustard to its related nontoxic sulfoxide. The same complex was used as catalyst for two model oxidative C–C coupling reactions, namely, the coupling of aryl diazonium salts with alkynylsilanes and with mesitylene. These two catalytic reactions are a good indication that the (NDI-NHC)-Au(I) complex can behave as an effective dual metallaphotoredox catalyst but with the particular feature that both the photosensitizer and the metal catalyst are contained in the same compound, thus constituting a very rare type of a “two-in-one” metallaphotoredox catalyst. The participation of the Au(I)/Au(III) couple in the catalytic process was demonstrated by the isolation of a Au(III) complex, which was obtained via a self-photoactivated photoredox reaction.

KEYWORDS: gold, metallaphotoredox, two-in-one photocatalyst, singlet oxygen, endoperoxidation, C–C coupling, N-heterocyclic carbene

INTRODUCTION

During the past three decades, the use of catalysts with ligands that incorporate stimulus-responsive units has appeared as an efficient way of conferring a biomimetic level of control over chemical transformations.¹ Such level of control allows the tuning of the catalyst for specific needs and therefore can be used to enable chemical transformations that are difficult to achieve by other means. At the same level of catalyst design, dual catalysis has emerged as one of the most powerful strategies for the development of chemical reactions. Dual catalysis refers to a type of plural catalysis that combines the synergistic action of two catalysts² and provides a relatively simple strategy for the development of reactions that are normally inefficiently performed by a single catalyst. Metallaphotocatalysis is a special type of dual catalysis in which one catalyst is used to absorb light and harvest energy, and a second independent catalyst is used to manipulate the reactivity of the resulting photoexcited species.³ Recently, several visible light-absorbing metal complexes have shown to be active in bond-breaking and bond-forming events without the need of exogenous photosensitizers, but most of the times, these single-catalyst strategies are metal-dependent and normally require the use of highly sophisticated ligands.⁴

These catalysts operate via a single catalytic cycle, where the metal-based catalyst plays a dual duty by harvesting light and then enabling bond forming/breaking events. The use of a single catalyst framework has the advantage that the light energy can be more efficiently utilized than in dual-catalyst systems due to the intramolecular electron/energy transfer process. In addition, the efficiency of the reaction can be improved because the metal center neighbors the radicals that are formed, thus enhancing the connection between light, photosensitizer, and metal. In this context, only very recently, several authors have developed metal complexes with photoactive ligands to develop a new class of “two-in-one” metallaphotoredox cross-coupling catalysts.⁵ Some recent examples reported so far include the use of an acridine–palladium complex used for the cross-coupling of aryl halides with carboxylic acids,^{5c} the use of a nickel complex with a

Received: December 7, 2023

Revised: February 13, 2024

Accepted: February 14, 2024

Published: February 29, 2024



diarylquinolinium-embedded bipyridine ligand for the cross-coupling of aryl halides and organoboron compounds,^{5b} and the use of a palladium complex for promoting radical cross-coupling reactions.^{5a}

During the past decade, the combination of photocatalysis with gold catalysis has helped span the scope of gold catalysis far beyond the conventional π -activation of C–C unsaturated bonds. This combination of light and gold allows the use of gold catalysts for tandem nucleophilic additions/oxidative cross-coupling reactions without the use of strong external oxidants, which are normally required for facilitating the Au(I)/Au(III) oxidation step.⁶ It needs to be noted that important advances have been recently accomplished⁷ for oxidant-free C–C oxidative coupling reactions with aryl halides, which are facilitated by gold(I) catalysts by either using a directing group or by utilizing special bidentate ligands. The combination of a gold(I) complex with a photocatalyst is an interesting alternative because redox events can be easily achieved via electron transfer and radical addition at the gold center, thus opening the door to challenging redox Au(I)/Au(III) catalysis.⁸

We recently described the preparation of a series of rhodium, iridium,⁹ and gold¹⁰ complexes with naphthalene-diimide-decorated N-heterocyclic carbene ligands (NDI-NHCs), which we used as redox switchable catalysts for a number of organic transformations. For the design of these catalysts, we benefited from the reversibility of the two sequential one-electron reduction events at the NDI moiety to induce changes in the electron-donating strength of the NDI-NHC ligand, which were translated in the modification of the catalytic performances of the metal complexes. Together with the interesting electrochemical properties, NDIs can display excellent photochemical properties that may have the potential for being further applied for catalytic purposes, although these have been scarcely explored.¹¹ For example, NDIs combine intense light absorption, high stability, electron-accepting ability and high fluorescence quantum yields.¹² With these precedents in hand, in the study that we report herein, we sought to benefit from merging the catalytic activity of the gold center with the photochemical properties derived from the NDI moiety in the NDI-decorated NHC ligand. Since complex **1** (Figure 1) has an NDI moiety attached to the backbone of the NHC ligand, we thought that this could be used for promoting dual metallaphotocatalytic reactions without the requirement of adding an external photosensitizer. As will be described in the following sections of this manuscript, we herein describe the (i) ligand-centered photocatalytic properties of the NDI-NHC–Au–Cl complex **1**, (ii) its ability to promote the photochemical oxidation of Au(I) to Au(III), and (iii) its ability to facilitate catalytic oxidative C–C coupling reactions using aryl-diazonium salts.

RESULTS AND DISCUSSION

Figure 1 shows the UV–vis spectra of **1** and the NDI-imidazolium salt **A**, which was used as an NHC precursor in the preparation of **1**. Both spectra show strong NDI-centered vibronically structured bands with λ_{max} at 450 and 545 nm, for **A** and **1**, respectively. The red-shifted absorption of complex **1** with respect to that observed for the imidazolium salt **A** is a consequence of the combined effect of the coordination of the gold atom and the disappearance of the positive charge.

One of the most interesting photochemical properties of NDI-containing compounds is their ability to behave as singlet

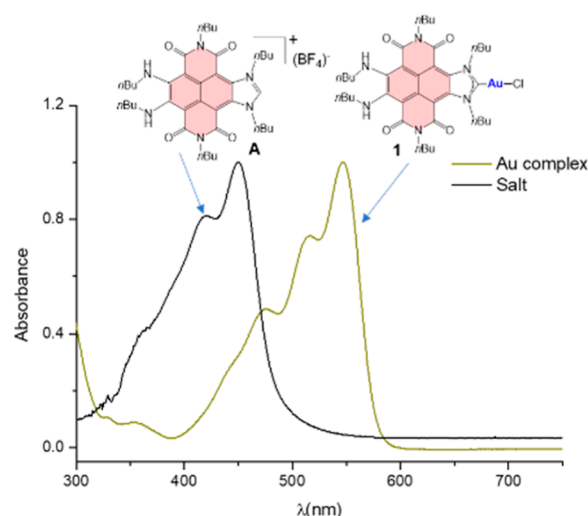


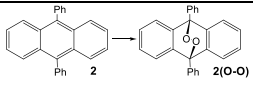
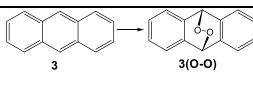
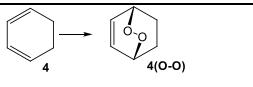
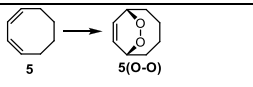
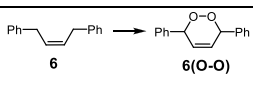
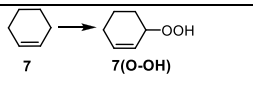
Figure 1. UV–vis spectra of the imidazolium salt **A** and gold complex **1** in CH_2Cl_2 ($50 \mu\text{M}$, 25°C).

oxygen ($^1\text{O}_2$) photosensitizers.¹³ Given the strong absorption of complex **1** in the visible region, we sought to test if our gold(I) complex would be an efficient $^1\text{O}_2$ photosensitizer and, if so, if it could be used for the photocatalytic peroxidation of organic molecules. The endoperoxidation of alkenes is a very interesting reaction because many endoperoxides are biological active reagents¹⁴ that are often used in a large number of organic transformations.¹⁵ In addition, the reactions of alkenes and dienes with singlet oxygen are receiving increasing attention due to the interest in finding biomimetic routes to natural products.¹⁶ As a model reaction, we first studied the endoperoxidation of 9,10-diphenylanthracene (DPA). The reaction was carried out at room temperature using a 2 mM solution of DPA in acetonitrile and 4×10^{-3} mM of **1**, irradiating with a household light-emitting diode (LED) lamp at 527 nm, with $5.2 \text{ mW}/\text{cm}^2$ of incident power. Under these reaction conditions, we observed that the resulting anthracenyl-endoperoxide was obtained quantitatively in just 30 min. By comparing the time-dependent reaction profiles of the endoperoxidation of DPA with **1** with the reaction profile resulting from the reaction carried out with Rose Bengal (singlet oxygen quantum yield = $\phi_{\Delta} = 0.53$),¹⁷ we were able to determine the singlet oxygen quantum yield of **1**, $\phi_{\Delta(1)} = 0.93$ (details on the calculation can be found in Pages S5–S6 in the Supporting Information), thus surpassing the best results reported in previous studies for NDI-containing photosensitizers.^{13,18} It is also important to point out that the NDI-imidazolium salt **A** that is used as the NHC ligand precursor in the synthesis of **1** did not show any activity in the endoperoxidation of DPA under these reaction conditions as it should be expected due to the negligible absorbance shown by this compound at 527 nm. Interestingly, when **A** was used and the irradiation was carried out at 450 nm (where **A** shows its maximum absorption), the amount of diphenylanthracene endoperoxide formed was also negligible (<10%).

We next decided to explore the substrate scope of the reaction, for which a series of cyclic and acyclic alkenes were subjected to irradiation in the presence of **1**. For these reactions, we used six different substrates in order to compare their reactivity and to explore their tolerance to functional groups. In particular, substrates **2–5** are known to react with singlet oxygen via a photoinduced Diels–Alder reaction in

which singlet oxygen is the dienophile. As can be observed from the data shown in Table 1, substrates 2–5 reacted with

Table 1. Peroxidation of Organic Substrates by Light-Induced Cycloaddition of $^1\text{O}_2$ ^a

Entry	Substrate/Product	Time	Yield (%) ^b
1		10 min	>99
2 ^c		30 min	>99
3		1h	>99
4		12h	70
5		4h	88
6		24h	66

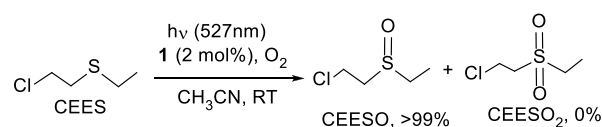
^aReactions carried out in CD_3CN in a nuclear magnetic resonance (NMR) tube with 2 mM of substrate under O_2 atmosphere, using 0.02 mM (1 mol %) of **1**. ^bProton NMR (^1H NMR) yields, using anisole (2 mM) as internal integration standard. Samples were irradiated with an LED lamp at 527 nm (5.2 mW/cm²). ^c0.2 mol % of **1** was used.

singlet oxygen, affording the corresponding endoperoxidation products in very high yield. In the case of anthracene, the formation of anthracenyl-endoperoxide (**3(O–O)**) was quantitative in half an hour using only 0.2 mol % of photocatalyst (entry 2). The reaction of cyclohexene produced cyclohexenyl hydroperoxide (**7(O–OH)**) in 66% yield after 24 h of reaction (entry 6). This product is formed through an *ene* reaction, yielding an allylic hydroperoxide in which the double bond of the substrate has been shifted to a position adjacent to the original double bond.¹⁹

Encouraged by these results, we wondered whether complex **1** could also be used for the detoxification of bis(2-chloroethyl)sulfide, more widely known as sulfur mustard. Although several methods have been used for the detoxification of sulfur mustard (incineration, hydrolysis, oxidation, and dehydrohalogenation),²⁰ these have shown to be rather ineffective and also pose great risk to humans if the agents are not completely degraded. As a result, partial oxidation of sulfur mustard to bis(2-chloroethyl)sulfoxide is considered to be the most convenient detoxification route, since the overoxidized sulfone product is just as toxic as sulfur mustard itself.^{20a} One way to control the selective oxidation of the sulfide to the sulfoxide is to use a mild oxidant, for which the use of singlet oxygen is now considered as one of the most promising methods for selective partial oxidation of sulfur mustard.²¹ Given the high efficiency of **1** in the generation of singlet oxygen, we decided to test our complex in the oxidation of 2-

chloroethyl ethyl sulfide (CEES), one of the most commonly used simulants for sulfur mustard (Scheme 1).²² The reaction

Scheme 1. Oxidation of CEES to CEESO Using Singlet Oxygen Produced by the Photosensitizer **1**

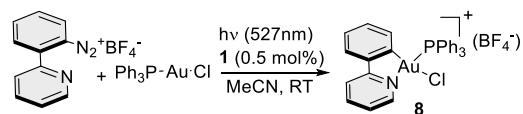


was performed in acetonitrile, with a 2 mol % of **1**, using a LED lamp at 527 nm, under an O_2 atmosphere. We observed that after 20 min, CEES was quantitatively converted into chloroethyl ethyl sulfoxide (CEESO). Under the reaction conditions used, we did not observe the formation of 2-chloroethyl ethyl sulfone (CEESO₂), which could have been produced from the overoxidation of CEES, thus indicating the high selectivity of the reaction toward the partially oxidized nontoxic product, CEESO.

The generation of $^1\text{O}_2$ with a photosensitizer is normally produced via an energy transfer process. In our case, the NDI moiety of the ligand is used as a triplet sensitizer for photooxidation (via sensitizing singlet oxygen), and the process occurs via a triplet–triplet energy-transfer (TTET). For this type of photocatalytic process, the electrochemical potentials are not useful predictors of reactivity, while the relative triplet-state energy for the photocatalyst and substrate are the most important parameters for determining the feasibility of the energy transfer. For photoredox processes, the feasibility of the reaction is primarily determined by the relative half potentials of the photocatalyst in its excited state and the substrate. In the case of **1**, cyclic voltammetry shows two reversible reductions and one irreversible oxidation (see the Supporting Information file for full details). The two reductions are assigned to the formation of the radical monoanion $\mathbf{1}^{\bullet-}$ [$E_{1/2} = -0.82$ V vs saturated calomel electrode (SCE)] and the dianion $\mathbf{1}^{2-}$ ($E_{1/2} = -1.3$ V vs SCE). The oxidation observed at $E_{1/2}(\mathbf{1}^{\bullet+}/\mathbf{1}) = 1.31$ V can be related to the electron-donating effect exerted by the N-nBu groups at the core.¹¹ The key values for the photoredox activity of **1** are the excited-state potential for the reduction $E_{\text{red}}^*(\mathbf{1}^{\bullet+}/\mathbf{1}^{\bullet-}) = 1.34$ V and for the oxidation $E_{\text{ox}}^*(\mathbf{1}^{\bullet+}/\mathbf{1}) = -0.86$ V, which can be obtained combining the electrochemical and spectroscopic properties of the complex using the Rehm–Weller theory.²³ These values indicate that **1** in the excited state is a strong oxidant and a mild reductant and suggest that the complex could be used as a photosensitizer in reactions typically facilitated by the ubiquitous photocatalyst $[\text{Ru}(\text{bpy})_3]^{2+}$ [$\text{Ru}(\text{II})^*/\text{Ru}(\text{I}) = 0.77$ V; $\text{Ru}(\text{III})^*/\text{Ru}(\text{II}) = -0.81$ V vs SCE; $\lambda_{\text{max}} = 452$ nm].

With these data in hand, we decided to study the oxidative addition of 2-(pyridin-2-yl)benzenediazonium tetrafluoroborate to $[\text{AuCl}(\text{PPh}_3)]$ (Scheme 2). This reaction constitutes a

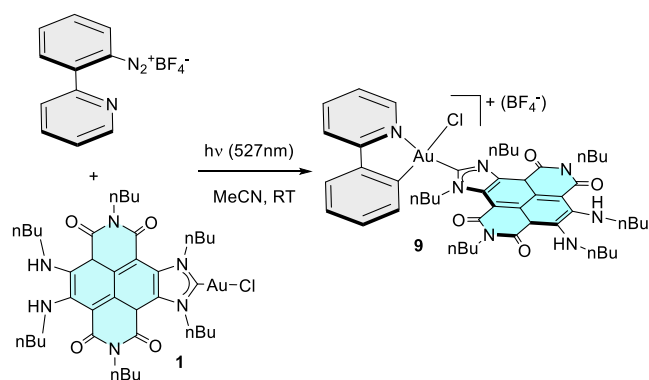
Scheme 2. Photoredox-Promoted Oxidative Addition of an Aryldiazonium Salt to $[\text{AuCl}(\text{PPh}_3)]$ Using **1 as Photocatalyst**



very interesting example of a visible-light-promoted photoredox method for the oxidative addition of aryldiazonium salts to gold(I) complexes and is performed using $[\text{Ru}(\text{bpy})_3](\text{BF}_4)_2$ as the photosensitizer.²⁴ In order to study if the same reaction could be performed using **1** as the photosensitizer, we carried out the reaction between $[\text{AuCl}(\text{PPh}_3)]$ and the aryldiazonium salt in acetonitrile at room temperature, using 0.5 mol % of **1**, and irradiated the solution with an LED light ($\lambda = 527 \text{ nm}$) during 3 h. Under these reaction conditions, we obtained the corresponding Au(III) complex **8** in 87% isolated yield, a result that outperforms the previously published result using $[\text{Ru}(\text{bpy})_3](\text{BF}_4)_2$,²⁴ for which 80% of the Au(III) product was obtained after 4 h of reaction.

Given that **1** is a Au(I) complex itself, we also performed the direct reaction of **1** with the aryldiazonium salt in acetonitrile under visible light irradiation and observed that the new Au(III) complex **9** was obtained quantitatively after 3 h (Scheme 3). Complex **9** was characterized by nuclear magnetic

Scheme 3. Self-Photoredox-Promoted Oxidative Addition of an Aryldiazonium Salt to **1**



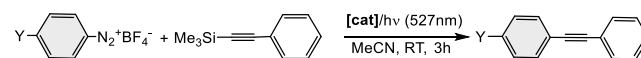
resonance (NMR) spectroscopy and electrospray ionization mass spectrometry (ESI-MS) (see the Supporting Information for full details). This reaction is very interesting because the oxidation of Au(I) to Au(III) is produced without the need of adding an external photosensitizer and therefore can be regarded as a very rare case of a self-photoactivated photoredox reaction, but most importantly, it indicates that complex **1** is suitable for participating in Au(I)/Au(III) photoredox events.

Both reactions shown in Schemes 2 and 3 prompted us to use **1** as a (single) dual photoredox catalyst for C–C coupling reactions involving aryldiazonium salts.²⁵ The use of **1** in this type of reaction would benefit from the fact that the reactions could be performed without the need of the addition of an external photosensitizer, thus producing a series of significant advantages, such as (i) the reduction in the cost of the reaction setup, (ii) the simplification of the reaction workup, and (iii) the performance of the reaction in a more sustainable manner as smaller amounts of metal-containing additives would be needed for facilitating the reaction. More importantly, the fact that both the photosensitizer and the metal catalyst are contained in the same framework may enhance the efficiency of the electron transfer during the catalytic cycle, and this may have benefits regarding the activity of the catalytic process.

As a first model reaction, we chose to study the coupling of alkynyl-silanes with aryldiazonium salts,²⁶ a reaction that exemplifies the participation of Au(I)/Au(III) cycles facilitated by a photoredox catalyst. We performed the reaction between

four different aryldiazonium tetrafluoroborates and trimethylsilylethynylbenzene in acetonitrile at room temperature, under irradiation with an LED light ($\lambda = 527 \text{ nm}$), using 10 mol % of **1**. For comparative purposes, we also performed the reaction using $[\text{AuCl}(\text{PPh}_3)]$ (10 mol %) and $[\text{Ru}(\text{bpy})_3](\text{PF}_6)_2$ (0.5 mol %) under the same conditions. As can be observed from the data shown in Table 2, catalyst **1** is a suitable catalyst for

Table 2. Dual Gold Photoredox Coupling of Aryldiazonium Tetrafluoroborates and Trimethylsilylethynylbenzene^a



Y = H, NO₂, F, CF₃

entry	Y	catalyst	yield (%) ^b
1	H	1	60
2	H	$[\text{AuCl}(\text{PPh}_3)] + [\text{Ru}(\text{bpy})_3]^{2+}$	58
3	NO ₂	1	74
4	NO ₂	$[\text{AuCl}(\text{PPh}_3)] + [\text{Ru}(\text{bpy})_3]^{2+}$	59
5	F	1	66
6	F	$[\text{AuCl}(\text{PPh}_3)] + [\text{Ru}(\text{bpy})_3]^{2+}$	60
7	CF ₃	1	60
8	CF ₃	$[\text{AuCl}(\text{PPh}_3)] + [\text{Ru}(\text{bpy})_3]^{2+}$	52

^aReaction conditions: Reactions were carried out in CD₃CN at room temperature during 3 h, using a 10 mol % of gold catalyst with respect to limiting reagent. For the reactions carried out with $[\text{AuCl}(\text{PPh}_3)]$, 0.5 mol % of the Ru-photosensitizer was added. Samples were irradiated with an LED lamp at 527 nm (5.2 mW/cm²). ^bIsolated yields, average of two experiments. All other specific details can be found in the Supporting Information file.

this C–C coupling reaction, allowing the formation of the final products in yields ranging from 60 to 74%. Probably more interesting is the fact that catalyst **1** consistently outperforms the activity shown by the mixture of $[\text{AuCl}(\text{PPh}_3)]$ and $[\text{Ru}(\text{bpy})_3](\text{PF}_6)_2$ under the same reaction conditions. It is also important to point out that the reaction is carried out employing green light, which is of lower energy than that of the blue light that is normally used for promoting this type of C–C coupling. For further comparative purposes, we also performed the reaction using $[\text{AuCl}(\text{PPh}_3)]$ and $[\text{Ru}(\text{bpy})_3](\text{PF}_6)_2$ under blue light irradiation (450 nm) and observed that under these conditions, the product yield was, again, 58%, thus the same as that reported in the literature for this reaction.²⁶

In order to get a better insight on the different catalytic behaviors of **1** and the $[\text{AuCl}(\text{PPh}_3)]/[\text{Ru}(\text{bpy})_3](\text{PF}_6)_2$ catalytic mixture, we decided to monitor the evolution of the coupling of *p*-nitrophenyldiazonium tetrafluoroborate with trimethylsilylethynylbenzene using both catalysts. The reactions were carried out in CD₃CN in an NMR tube, using 7.5 mol % of Au catalysts, and 0.4 mol % of $[\text{Ru}(\text{bpy})_3](\text{PF}_6)_2$ for the case that $[\text{AuCl}(\text{PPh}_3)]$ was used (see Pages S12–S14 in the Supporting Information for full details). For these experiments, we decided to irradiate with white light, in order to ensure that both photosensitizers are illuminated at their maximum absorbance wavelengths. The resulting reaction profiles are shown in Figure 2. As can be observed from the profiles, catalyst **1** not only outperforms the activity of $[\text{AuCl}(\text{PPh}_3)] + [\text{Ru}(\text{bpy})_3](\text{PF}_6)_2$ all along the reaction profile but also produces a higher final product yield (90% vs 70%, both with 100% of substrate conversion). It is worth noting that, under these reaction conditions, the reaction is more effective than that shown in entries 3 and 4 in Table 2 as

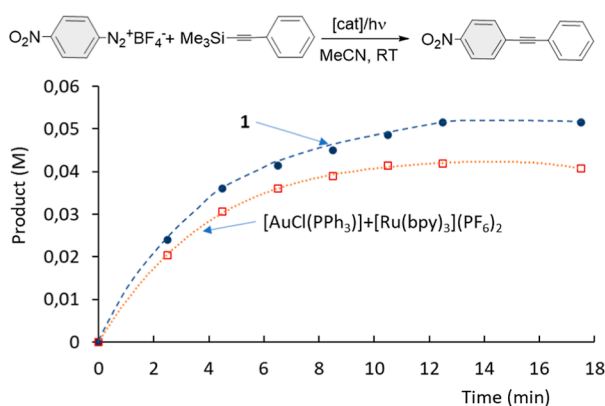


Figure 2. Time-dependent reaction profiles of the coupling of *p*-nitrophenyldiazonium tetrafluoroborate with trimethylsilylethynylbenzene with **1** (blue dots) and $[\text{AuCl}(\text{PPh}_3)] + [\text{Ru}(\text{bpy})_3](\text{PF}_6)_2$ (orange squares). The reactions were carried out in CD_3CN at room temperature using a 20 W white LED lamp. The initial concentration of both substrates was 0.06 M. The concentration of the Au catalyst was 7.5 mol %. The concentration of $[\text{Ru}(\text{bpy})_3](\text{PF}_6)_2$ was 0.4 mol %.

it reaches completion in less than 20 min with a lower catalyst loading. This is most likely due to the higher concentration of catalyst and substrates used for this experiment, together with the fact that the samples are irradiated with the whole window of wavelengths in the visible region as a white lamp was used.

In order to see if the good activity of catalyst **1** could be extended to other metallophotoredox-promoted reactions, we also studied the coupling of aryldiazonium tetrafluoroborates and mesitylene. This cross-coupling reaction proceeds via direct C–H activation of mesitylene and would normally require strong oxidants, but it was recently shown to be feasible via dual gold photoredox catalysis.²⁷ For testing this reaction, we performed the reactions in acetonitrile at room temperature under green light irradiation using 10 mol % of catalyst **1**. Again, for comparative purposes, we also carried out the reactions using $[\text{AuCl}(\text{PPh}_3)]$ (10 mol %) and $[\text{Ru}(\text{bpy})_3](\text{PF}_6)_2$ (0.5 mol %) under the same conditions. As can be observed from the data shown in Table 3, under these reaction

Table 3. Dual Gold Photoredox Coupling of Aryldiazonium Tetrafluoroborates and Mesitylene^a

entry	Y	catalyst	yield (%) ^b
1	NO ₂	1	67
2	NO ₂	$[\text{AuCl}(\text{PPh}_3)] + [\text{Ru}(\text{bpy})_3]^{2+}$	57
3	F	1	90
4	F	$[\text{AuCl}(\text{PPh}_3)] + [\text{Ru}(\text{bpy})_3]^{2+}$	79
5	CF ₃	1	34
6	CF ₃	$[\text{AuCl}(\text{PPh}_3)] + [\text{Ru}(\text{bpy})_3]^{2+}$	21

^aReaction conditions: Reactions were carried out in CD_3CN at room temperature for 3 h, using a 10 mol % of gold catalyst with respect to limiting reagent. For the reactions carried out with $[\text{AuCl}(\text{PPh}_3)]$, 0.5 mol % of the Ru-photosensitizer was added. Samples were irradiated with an LED lamp at 527 nm (5.2 mW/cm²). ^bYields are an average of two experiments and were calculated by ¹H NMR using trimethoxybenzene as standard.

conditions, the activity of **1** is significantly and consistently higher than the activity shown by the conventional $[\text{AuCl}(\text{PPh}_3)]/[\text{Ru}(\text{bpy})_3](\text{PF}_6)_2$ mixture and even outperforms some of the previously reported results for the coupling of these two types of substrates.²⁷ Again, we also tried the reaction using the $[\text{AuCl}(\text{PPh}_3)]/[\text{Ru}(\text{bpy})_3](\text{PF}_6)_2$ mixture for the coupling of *p*-nitrophenyldiazonium tetrafluoroborate with mesitylene and obtained a product yield of 57%, which is the same as the one reported in the literature for the coupling of these two substrates.²⁷

In order to check if the better activity of catalyst **1** was maintained all along the reaction course, we also time-monitored the coupling of *p*-nitrophenyldiazonium tetrafluoroborate with mesitylene. The reactions were performed in an NMR tube, using 7.5 mol % of Au catalysts and 0.4 mol % of $[\text{Ru}(\text{bpy})_3](\text{PF}_6)_2$ (for the case of $[\text{AuCl}(\text{PPh}_3)]$), and the samples were irradiated with white light (see Pages S15–S17 in the Supporting Information for full details). The resulting reaction profiles are shown in Figure 3. As can be observed

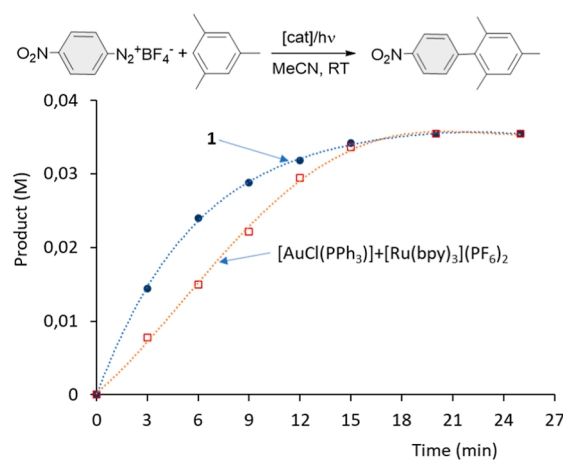
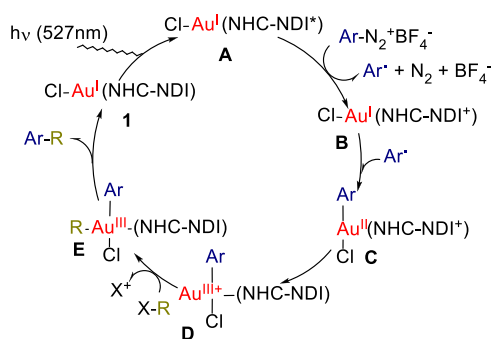


Figure 3. Time-dependent reaction profiles of the coupling of *p*-nitrophenyldiazonium tetrafluoroborate with mesitylene with **1** (blue dots) and $[\text{AuCl}(\text{PPh}_3)] + [\text{Ru}(\text{bpy})_3](\text{PF}_6)_2$ (orange squares). The reactions were carried out in CD_3CN at room temperature using a 20 W white LED lamp. The initial concentration of *p*-nitrophenyldiazonium tetrafluoroborate was 0.06 M, and a 6-fold excess of mesitylene was used. The concentration of the Au catalyst was 7.5 mol %. The concentration of $[\text{Ru}(\text{bpy})_3](\text{PF}_6)_2$ was 0.4 mol %.

from the comparison of the profiles, the activity of **1** is higher than that shown for the $[\text{AuCl}(\text{PPh}_3)] + [\text{Ru}(\text{bpy})_3](\text{PF}_6)_2$ system all along the reaction profile. The comparison of the initial rates (taken after 3 min of reaction) indicates that the reaction using **1** is 1.9 times faster than the reaction performed with the Au/Ru bimetallic system. Again, under these reaction conditions, the process is more efficient than when the conditions are those used for the construction of the data shown in Table 3. The reasons for this higher efficiency are the same as those explained before.

Based on other studies on Au-photoredox catalysis involving aryldiazonium salts,^{27,28} we hypothesized a mechanism involving the Au(I)/Au(III) cycle that is shown in Scheme 4. Irradiation of **1** with visible light generates $[\text{ClAu}^{\text{I}}(\text{NHC-NDI}^*)]$ (**A**), in which the NDI moiety of the ligand is photoexcited. Then, this species reacts with $\text{Ar-N}_2^+\text{BF}_4^-$, via a single-electron transfer process (SET), generating the neutral radical Ar^\bullet , which adds to the resulting $[\text{ClAu}^{\text{I}}(\text{NHC-NDI}^*)]$

Scheme 4. Proposed Metallaphotoredox Catalytic Cycle Involving Catalyst 1



(B) to generate the gold(II) cationic species $[\text{ClAu}^{\text{II}}(\text{Ar})(\text{NHC-NDI}^+)]$ (C), in which the NDI moiety of the NHC ligand is oxidized. This species undergoes intramolecular SET between the oxidized NDI moiety and the gold(II) atom to generate $[\text{ClAu}^{\text{III}}(\text{Ar})(\text{NHC-NDI})]^+$ (D), with an electrophilic Au(III) center. It is important to point out that this SET process proceeds via an inner-sphere mechanism, which is uncommon in conventional photoredox catalysis. Then, D reacts with a nucleophilic organic substrate (R-X) to generate the σ -bound tetracoordinated Au(III) intermediate $[\text{ClAu}^{\text{III}}(\text{Ar})(\text{R})(\text{NHC-NDI})]$ (E). In the final step of the cycle, E reductively eliminates Ar-R-regenerating Au(I) catalyst 1. We think that this mechanism may also explain the higher efficiency of complex 1 in metallaphotoredox catalysis compared with those of other dual catalytic systems. First, the generation of the aryl radical via the SET process to the aryldiazonium salt is produced next to the gold center, thus facilitating its rapid coordination, compared to the situation in which an external photocatalyst is used, and thus the aryl radical is generated far from the Au(I) center. Second, the fact that the SET between the oxidized NDI moiety and the Au(II) center ($[\text{ClAu}^{\text{II}}(\text{Ar})(\text{NHC-NDI})] \rightarrow [\text{ClAu}^{\text{III}}(\text{Ar})(\text{NHC-NDI})]^+$) is intramolecular (instead of intermolecular as in the case that an external photocatalyst is used) should also enhance the efficiency of this step of the process.

CONCLUSIONS

We showed that the $[\text{AuCl}(\text{NHC-NDI})]$ complex 1, is a versatile catalyst, which can participate in a number of photocatalytic reactions. The presence of the photoactive NDI moiety attached to the NHC ligand makes this complex suitable for the photogeneration of singlet oxygen and thus to behave as an effective catalyst in the endoperoxidation and peroxidation of cyclic and acyclic alkenes and also in the selective oxidation of CEES to the nontoxic product CEESO. We also proved that complex 1 can substitute the ubiquitous photosensitizer $[\text{Ru}(\text{bpy})_3]^{2+}$, in a number of photocatalytic reactions, thus indicating that this catalyst can participate both in TTET events (as in the processes involving the generation of singlet oxygen) and in photoredox catalysis (as in the generation of the Au(III) complex 9 shown in Scheme 3). However, all these reactions can be regarded as ligand-centered processes, in which the participation of the gold center is limited to red-shifting the maximum absorbance of the complex, so that it can be photoactive when excited in the visible region. For further exploration of the catalytic features of 1, we then merged the ligand-centered photoredox properties of the complex with the metal-centered catalytic

properties derived from the presence of the gold(I) atom. We found that 1 is an efficient catalyst for a variety of oxidative C–C coupling reactions, including the coupling of aryldiazonium salts with alkynylsilanes and mesitylene, with the latter one involving direct C–H activation of arenes under very mild reaction conditions. The fact that 1 can promote these variety of dual gold-photoredox catalytic processes constitutes a clear benefit with respect to previously reported examples of dual gold-based metallaphotoredox processes because complex 1 is able to facilitate these couplings without the need of addition of an external photoredox catalyst. We consider very meaningful the fact that a single catalyst like 1 is able to not only compare but also outperform other dual gold-based metallaphotoredox systems reported previously. The use of a single catalyst for dual metallaphotoredox catalysis simplifies the reaction workup, enhances the atom economy of the reactions, and makes gold-based oxidative C–C couplings more sustainable. To the best of our knowledge, no other gold(I) catalysts reported to date show the catalytic features shown by 1.

ASSOCIATED CONTENT

Supporting Information

The Supporting Information is available free of charge at <https://pubs.acs.org/doi/10.1021/acscatal.3c05962>.

Experimental details concerning all catalytic studies including all NMR spectra and electro-spectrochemical characterization of new complexes (PDF)

AUTHOR INFORMATION

Corresponding Authors

Macarena Poyatos – *Institute of Advanced Materials (INAM), Centro de Innovación en Química Avanzada (ORFEO-CINQA), Universitat Jaume I, Castellón E-12071, Spain*; orcid.org/0000-0003-2000-5231; Email: poyatosd@uji.es

Eduardo Peris – *Institute of Advanced Materials (INAM), Centro de Innovación en Química Avanzada (ORFEO-CINQA), Universitat Jaume I, Castellón E-12071, Spain*; orcid.org/0000-0001-9022-2392; Email: eperis@uji.es

Author

César Ruiz-Zambrana – *Institute of Advanced Materials (INAM), Centro de Innovación en Química Avanzada (ORFEO-CINQA), Universitat Jaume I, Castellón E-12071, Spain*; orcid.org/0000-0003-4208-0929

Complete contact information is available at: <https://pubs.acs.org/doi/10.1021/acscatal.3c05962>

Notes

The authors declare no competing financial interest.

ACKNOWLEDGMENTS

We gratefully acknowledge the financial support from the Ministerio de Ciencia y Universidades (PID2021-127862NB-I00), Generalitat Valenciana (CIPROM/2021/079), and the Universitat Jaume I (UJI-B2020-01 and UJI-B2021-39). We are grateful to the Serveis Centrals d'Instrumentació Científica (SCIC-UJI) for providing with spectroscopic facilities.

REFERENCES

- (1) (a) Crabtree, R. H. Multifunctional ligands in transition metal catalysis. *New J. Chem.* **2011**, *35*, 18–23. (b) Berben, L. A.; de Bruin, B.; Heyduk, A. F. Non-innocent ligands. *Chem. Commun.* **2015**, *51*, 1553–1554. (c) Lyaskovskyy, V.; de Bruin, B. Redox Non-Innocent Ligands: Versatile New Tools to Control Catalytic Reactions. *ACS Catal.* **2012**, *2*, 270–279. (d) Hindson, K.; de Bruin, B. Special Issue: Cooperative & Redox Non-Innocent Ligands in Directing Organometallic Reactivity (Cluster Issue). *Eur. J. Inorg. Chem.* **2012**, *2012*, 340–342. (e) Luning, U. Switchable Catalysis. *Angew. Chem., Int. Ed.* **2012**, *51*, 8163–8165. (f) Blanco, V.; Leigh, D. A.; Marcos, V. Artificial switchable catalysts. *Chem. Soc. Rev.* **2015**, *44*, 5341–5370. (g) Choudhury, J. Recent developments on artificial switchable catalysis. *Tetrahedron Lett.* **2018**, *59*, 487–495. (h) Bordet, A.; Leitner, W. Adaptive Catalytic Systems for Chemical Energy Conversion. *Angew. Chem., Int. Ed.* **2023**, *62*, No. e202301956.
- (2) (a) Kim, U. B.; Jung, D. J.; Jeon, H. J.; Rathwell, K.; Lee, S. G. Synergistic Dual Transition Metal Catalysis. *Chem. Rev.* **2020**, *120*, 13382–13433. (b) Malakar, C. C.; Dell'Amico, L.; Zhang, W. B. Dual Catalysis in Organic Synthesis: Current Challenges and New Trends. *Eur. J. Org. Chem.* **2023**, *26*, No. e202201114.
- (3) (a) Chan, A. Y.; Perry, I. B.; Bissonnette, N. B.; Buksh, B. F.; Edwards, G. A.; Frye, L. I.; Garry, O. L.; Lavagnino, M. N.; Li, B. X.; Liang, Y. F.; Mao, E.; Millet, A.; Oakley, J. V.; Reed, N. L.; Sakai, H. A.; Seath, C. P.; MacMillan, D. W. C. Metallaphotoredox: The Merger of Photoredox and Transition Metal Catalysis. *Chem. Rev.* **2022**, *122*, 1485–1542. (b) Twilton, J.; Le, C.; Zhang, P.; Shaw, M. H.; Evans, R. W.; MacMillan, D. W. C. The merger of transition metal and photocatalysis. *Nat. Rev. Chem.* **2017**, *1*, 0052. (c) Prier, C. K.; Rankic, D. A.; MacMillan, D. W. C. Visible Light Photoredox Catalysis with Transition Metal Complexes: Applications in Organic Synthesis. *Chem. Rev.* **2013**, *113*, 5322–5363.
- (4) (a) Parasram, M.; Gevorgyan, V. Visible light-induced transition metal-catalyzed transformations: beyond conventional photosensitizers. *Chem. Soc. Rev.* **2017**, *46*, 6227–6240. (b) Kancharla, R.; Muralirajan, K.; Sagadevan, A.; Rueping, M. Visible Light-Induced Excited-State Transition-Metal Catalysis. *Trends Chem.* **2019**, *1*, 510–523. (c) Cheung, K. P. S.; Sarkar, S.; Gevorgyan, V. Visible Light-Induced Transition Metal Catalysis. *Chem. Rev.* **2022**, *122*, 1543–1625.
- (5) (a) Kuribara, T.; Nakajima, M.; Nemoto, T. A visible-light activated secondary phosphine oxide ligand enabling Pd-catalyzed radical cross-couplings. *Nat. Commun.* **2022**, *13*, 4052. (b) Li, J. B.; Huang, C. Y.; Li, C. J. Two-in-one metallaphotoredox cross-couplings enabled by a photoactive ligand. *Chem* **2022**, *8*, 2419–2431. (c) Toriumi, N.; Inoue, T.; Iwasawa, N. Shining Visible Light on Reductive Elimination: Acridine-Pd-Catalyzed Cross-Coupling of Aryl Halides with Carboxylic Acids. *J. Am. Chem. Soc.* **2022**, *144*, 19592–19602.
- (6) (a) Akram, M. O.; Banerjee, S.; Saswade, S. S.; Bedi, V.; Patil, N. T. Oxidant-free oxidative gold catalysis: the new paradigm in cross-coupling reactions. *Chem. Commun.* **2018**, *54*, 11069–11083. (b) Nijamudheen, A.; Datta, A. Gold-Catalyzed Cross-Coupling Reactions: An Overview of Design Strategies, Mechanistic Studies, and Applications. *Chem.—Eur. J.* **2020**, *26*, 1442–1487. (c) Rocchigiani, L.; Bochmann, M. Recent Advances in Gold(III) Chemistry: Structure, Bonding, Reactivity, and Role in Homogeneous Catalysis. *Chem. Rev.* **2021**, *121*, 8364–8451. (d) Zheng, Z. T.; Wang, Z. X.; Wang, Y. L.; Zhang, L. M. Au-Catalyzed oxidative cyclisation. *Chem. Soc. Rev.* **2016**, *45*, 4448–4458. (e) Joost, M.; Amgoune, A.; Bourissou, D. Reactivity of Gold Complexes towards Elementary Organometallic Reactions. *Angew. Chem., Int. Ed.* **2015**, *54*, 15022–15045. (f) Font, P.; Ribas, X. Fundamental Basis for Implementing Oxidant-Free Au(I)/Au(III) Catalysis. *Eur. J. Inorg. Chem.* **2021**, *2021*, 2556–2569.
- (7) (a) Rigoulet, M.; Thillaye du Boullay, O.; Amgoune, A.; Bourissou, D. Gold(I)/Gold(III) Catalysis that Merges Oxidative Addition and pi-Alkene Activation. *Angew. Chem., Int. Ed.* **2020**, *59*, 16625–16630. (b) Joost, M.; Estevez, L.; Miqueu, K.; Amgoune, A.; Bourissou, D. Oxidative Addition of Carbon-Carbon Bonds to Gold. *Angew. Chem., Int. Ed.* **2015**, *54*, 5236–5240. (c) Joost, M.; Zeineddine, A.; Estevez, L.; Mallet-Ladeira, S.; Miqueu, K.; Amgoune, A.; Bourissou, D. Facile Oxidative Addition of Aryl Iodides to Gold(I) by Ligand Design: Bending Turns on Reactivity. *J. Am. Chem. Soc.* **2014**, *136*, 14654–14657. (d) Rodriguez, J.; Tabey, A.; Mallet-Ladeira, S.; Bourissou, D. Oxidative additions of alkynyl/vinyl iodides to gold and gold-catalyzed vinylation reactions triggered by the MeDalphos ligand. *Chem. Sci.* **2021**, *12*, 7706–7712. (e) Zeineddine, A.; Estevez, L.; Mallet-Ladeira, S.; Miqueu, K.; Amgoune, A.; Bourissou, D. Rational development of catalytic Au(I)/Au(III) arylation involving mild oxidative addition of aryl halides. *Nat. Commun.* **2017**, *8*, 565. (f) Harper, M. J.; Arthur, C. J.; Crosby, J.; Emmett, E. J.; Falconer, R. L.; Fensham-Smith, A. J.; Gates, P. J.; Leman, T.; McGrady, J. E.; Bower, J. F.; Russell, C. A. Oxidative Addition, Transmetalation, and Reductive Elimination at a 2,2'-Bipyridyl-Ligated Gold Center. *J. Am. Chem. Soc.* **2018**, *140*, 4440–4445. (g) Serra, J.; Parella, T.; Ribas, X. Au(III)-aryl intermediates in oxidant-free C-N and C-O cross-coupling catalysis. *Chem. Sci.* **2017**, *8*, 946–952.
- (8) (a) Hashmi, A. S. K. Dual Gold Catalysis. *Acc. Chem. Res.* **2014**, *47*, 864–876. (b) Skubi, K. L.; Blum, T. R.; Yoon, T. P. Dual Catalysis Strategies in Photochemical Synthesis. *Chem. Rev.* **2016**, *116*, 10035–10074. (c) Witzel, S.; Hashmi, A. S. K.; Xie, J. Light in Gold Catalysis. *Chem. Rev.* **2021**, *121*, 8868–8925. (d) Hopkinson, M. N.; Tlahuext-Aca, A.; Glorius, F. Merging Visible Light Photoredox and Gold Catalysis. *Acc. Chem. Res.* **2016**, *49*, 2261–2272. (e) Sahoo, B.; Hopkinson, M. N.; Glorius, F. Combining Gold and Photoredox Catalysis: Visible Light-Mediated Oxy- and Aminoarylation of Alkenes. *J. Am. Chem. Soc.* **2013**, *135*, 5505–5508.
- (9) (a) Ruiz-Zambrana, C.; Gutierrez-Blanco, A.; Gonell, S.; Poyatos, M.; Peris, E. Redox-Switchable Cycloisomerization of Alkynoic Acids with Naphthalenediimide-Derived N-Heterocyclic Carbene Complexes. *Angew. Chem., Int. Ed.* **2021**, *60*, 20003–20011. (b) Gutierrez-Pena, C. L.; Poyatos, M.; Peris, E. A redox-switchable catalyst with an 'unplugged' redox tag. *Chem. Commun.* **2022**, *58*, 10564–10567.
- (10) Ruiz-Zambrana, C.; Poyatos, M.; Peris, E. A redox-switchable gold(I) complex for the hydroamination of acetylenes: a convenient way for studying ligand-derived electronic effects. *ACS Catal.* **2022**, *12*, 4465–4472.
- (11) Reiß, B.; Wagenknecht, H. A. Naphthalene diimides with improved solubility for visible light photoredox catalysis. *Beilstein J. Org. Chem.* **2019**, *15*, 2043–2051.
- (12) (a) Feng, J. J.; Jiang, W.; Wang, Z. H. Synthesis and Application of Rylene Imide Dyes as Organic Semiconducting Materials. *Chem.—Asian J.* **2018**, *13*, 20–30. (b) Jiang, W.; Li, Y.; Wang, Z. H. Tailor-Made Rylene Arrays for High Performance n-Channel Semiconductors. *Acc. Chem. Res.* **2014**, *47*, 3135–3147. (c) Tovar, J. D. Supramolecular Construction of Optoelectronic Biomaterials. *Acc. Chem. Res.* **2013**, *46*, 1527–1537. (d) Maniam, S.; Higginbotham, H. F.; Bell, T. D. M.; Langford, S. J. Harnessing Brightness in Naphthalene Diimides. *Chem.—Eur. J.* **2019**, *25*, 7044–7057. (e) Kumar, S.; Shukla, J.; Kumar, Y.; Mukhopadhyay, P. Electron-poor arylenediimides. *Org. Chem. Front.* **2018**, *5*, 2254–2276. (f) Pan, M.; Lin, X. M.; Li, G. B.; Su, C. Y. Progress in the study of metal-organic materials applying naphthalene diimide (NDI) ligands. *Coord. Chem. Rev.* **2011**, *255*, 1921–1936. (g) Bhosale, S. V.; Jani, C. H.; Langford, S. J. Chemistry of naphthalene diimides. *Chem. Soc. Rev.* **2008**, *37*, 331–342. (h) Al Kobaisi, M.; Bhosale, S. V.; Latham, K.; Raynor, A. M.; Bhosale, S. V. Functional Naphthalene Diimides: Synthesis, Properties, and Applications. *Chem. Rev.* **2016**, *116*, 11685–11796. (i) Bhosale, S. V.; Al Kobaisi, M.; Jadhav, R. W.; Morajkar, P. P.; Jones, L. A.; George, S. Naphthalene diimides: perspectives and promise. *Chem. Soc. Rev.* **2021**, *50*, 9845–9998.
- (13) Guo, S.; Wu, W. H.; Guo, H. M.; Zhao, J. Z. Room-Temperature Long-Lived Triplet Excited States of Naphthalenediimides and Their Applications as Organic Triplet Photosensitizers for

- Photooxidation and Triplet-Triplet Annihilation Upconversions. *J. Org. Chem.* **2012**, *77*, 3933–3943.
- (14) (a) Meshnick, S. R.; Taylor, T. E.; Kamchonwongpaisan, S. Artemisinin and the antimalarial endoperoxides: From herbal remedy to targeted chemotherapy. *Microbiol. Rev.* **1996**, *60*, 301–315. (b) Moncada, S.; Vane, J. R. Pharmacology and Endogenous Roles of Prostaglandin Endoperoxides, Thromboxane-A₂, and Prostacyclin. *Pharmacol. Rev.* **1978**, *30*, 293–331.
- (15) Balci, M. Bicyclic Endoperoxides and Synthetic Applications. *Chem. Rev.* **1981**, *81*, 91–108.
- (16) (a) Ghogare, A. A.; Greer, A. Using Singlet Oxygen to Synthesize Natural Products and Drugs. *Chem. Rev.* **2016**, *116*, 9994–10034. (b) Di Mascio, P.; Martinez, G. R.; Miyamoto, S.; Ronsein, G. E.; Medeiros, M. H. G.; Cadet, J. Singlet Molecular Oxygen Reactions with Nucleic Acids, Lipids, and Proteins. *Chem. Rev.* **2019**, *119*, 2043–2086.
- (17) Epelde-Elezcano, N.; Martinez-Martinez, V.; Pena-Cabrera, E.; Gomez-Duran, C. F. A.; Arbeloa, I. L.; Lacombe, S. Modulation of singlet oxygen generation in halogenated BODIPY dyes by substitution at their meso position: towards a solvent-independent standard in the vis region. *RSC Adv.* **2016**, *6*, 41991–41998.
- (18) Doria, F.; Manet, I.; Grande, V.; Monti, S.; Freccero, M. Water-Soluble Naphthalene Diimides as Singlet Oxygen Sensitizers. *J. Org. Chem.* **2013**, *78*, 8065–8073.
- (19) Frimer, A. A. The reaction of singlet oxygen with olefins: the question of mechanism. *Chem. Rev.* **1979**, *79*, 359–387.
- (20) (a) Hirade, J.; Ninomiya, A. Studies on the Mechanism of the Toxic Action of Organic Halogen Compounds. *J. Biochem.* **1950**, *37*, 19–34. (b) Wagner, G. W.; Yang, Y. C. Rapid nucleophilic/oxidative decontamination of chemical warfare agents. *Ind. Eng. Chem. Res.* **2002**, *41*, 1925–1928. (c) Horcajada, P.; Surble, S.; Serre, C.; Hong, D. Y.; Seo, Y. K.; Chang, J. S.; Greneche, J. M.; Margiolaki, I.; Ferey, G. Synthesis and catalytic properties of MIL-100(Fe), an iron(III) carboxylate with large pores. *Chem. Commun.* **2007**, 2820–2822. (d) Talmage, S. S.; Watson, A. P.; Hauschild, V.; Munro, N. B.; King, J. Chemical warfare agent degradation and decontamination. *Curr. Org. Chem.* **2007**, *11*, 285–298. (e) Smith, B. M. Catalytic methods for the destruction of chemical warfare agents under ambient conditions. *Chem. Soc. Rev.* **2008**, *37*, 470–478. (f) Wang, Q.-Q.; Begum, R. A.; Day, V. W.; Bowman-James, K. Sulfur, oxygen, and nitrogen mustards: stability and reactivity. *Org. Biomol. Chem.* **2012**, *10*, 8786–8793.
- (21) (a) Liu, Y. Y.; Howarth, A. J.; Hupp, J. T.; Farha, O. K. Selective Photooxidation of a Mustard-Gas Simulant Catalyzed by a Porphyrinic Metal-Organic Framework. *Angew. Chem., Int. Ed.* **2015**, *54*, 9001–9005. (b) Liu, Y. Y.; Buru, C. T.; Howarth, A. J.; Mahle, J. J.; Buchanan, J. H.; DeCoste, J. B.; Hupp, J. T.; Farha, O. K. Efficient and selective oxidation of sulfur mustard using singlet oxygen generated by a pyrene-based metal-organic framework. *J. Mater. Chem. A* **2016**, *4*, 13809–13813. (c) Atilgan, A.; Islamoglu, T.; Howarth, A. J.; Hupp, J. T.; Farha, O. K. Detoxification of a Sulfur Mustard Simulant Using a BODIPY-Functionalized Zirconium-Based Metal-Organic Framework. *ACS Appl. Mater. Interfaces* **2017**, *9*, 24555–24560. (d) Liu, Y. Y.; Howarth, A. J.; Vermeulen, N. A.; Moon, S. Y.; Hupp, J. T.; Farha, O. K. Catalytic degradation of chemical warfare agents and their simulants by metal-organic frameworks. *Coord. Chem. Rev.* **2017**, *346*, 101–111. (e) Cao, M.; Pang, R.; Wang, Q. Y.; Han, Z.; Wang, Z. Y.; Dong, X. Y.; Li, S. F.; Zang, S. Q.; Mak, T. C. W. Porphyrinic Silver Cluster Assembled Material for Simultaneous Capture and Photocatalysis of Mustard-Gas Simulant. *J. Am. Chem. Soc.* **2019**, *141*, 14505–14509. (f) Oheix, E.; Gravel, E.; Doris, E. Catalytic Processes for the Neutralization of Sulfur Mustard. *Chem.—Eur. J.* **2021**, *27*, 54–68.
- (22) Kumar, V.; Anslyn, E. V. A selective and sensitive chromogenic and fluorogenic detection of a sulfur mustard simulant. *Chem. Sci.* **2013**, *4*, 4292–4297.
- (23) Buzzetti, L.; Crisenza, G. E. M.; Melchiorre, P. Mechanistic Studies in Photocatalysis. *Angew. Chem., Int. Ed.* **2019**, *58*, 3730–3747.
- (24) Tlahuext-Aca, A.; Hopkinson, M. N.; Daniliuc, C. G.; Glorius, F. Oxidative Addition to Gold(I) by Photoredox Catalysis: Straightforward Access to Diverse (C,N)-Cyclometalated Gold(III) Complexes. *Chem.—Eur. J.* **2016**, *22*, 11587–11592.
- (25) Mo, F. Y.; Qiu, D.; Zhang, L.; Wang, J. B. Recent Development of Aryl Diazonium Chemistry for the Derivatization of Aromatic Compounds. *Chem. Rev.* **2021**, *121*, 5741–5829.
- (26) Kim, S.; Rojas-Martin, J.; Toste, F. D. Visible light-mediated gold-catalysed carbon(sp²)-carbon(sp) cross-coupling. *Chem. Sci.* **2016**, *7*, 85–88.
- (27) Gauchot, V.; Sutherland, D. R.; Lee, A. L. Dual gold and photoredox catalysed C-H activation of arenes for aryl-aryl cross couplings. *Chem. Sci.* **2017**, *8*, 2885–2889.
- (28) (a) Tlahuext-Aca, A.; Hopkinson, M. N.; Sahoo, B.; Glorius, F. Dual gold/photoredox-catalyzed C(sp)-H arylation of terminal alkynes with diazonium salts. *Chem. Sci.* **2016**, *7*, 89–93. (b) Cornilleau, T.; Hermange, P.; Fouquet, E. Gold-catalysed cross-coupling between aryldiazonium salts and arylboronic acids: probing the usefulness of photoredox conditions. *Chem. Commun.* **2016**, 52, 10040–10043. (c) Shu, X. Z.; Zhang, M.; He, Y.; Frei, H.; Toste, F. D. Dual Visible Light Photoredox and Gold-Catalyzed Arylative Ring Expansion. *J. Am. Chem. Soc.* **2014**, *136*, 5844–5847. (d) Medina-Mercado, I.; Porcel, S. Insights into the Mechanism of Gold(I) Oxidation with Aryldiazonium Salts. *Chem.—Eur. J.* **2020**, *26*, 16206–16221.